

MODELLING OF HIGH-CYCLE FATIGUE CRACK GROWTH IN CONCRETE

JAN CERVENKA^{*}, ATHEER AL-SAOUDI[†] AND DOBROMIL PRYL^{*}

^{*} Cervenka Consulting s.r.o.
Prague, Czech Republic

E-mail: jan.cervenka@cervenka.cz
E-mail: dobromil.pryl@cervenka.cz

[†] Upper Lachlan Shire Council, NSW Government, Australia,
E-mail: atheeriq_2010@yahoo.co.uk

Key words: Fatigue Crack Growth, Finite Element Method, Concrete, FRP Strengthening

Abstract: This paper presents an advanced approach for modelling high-cycle fatigue in concrete structures without the need to model each individual cycle. The three-dimensional fracture-plastic model has been extended to capture fatigue damage in tension. The material model is based on the classical S-N or Wöhler curve. The S-N criterion is translated into a material damage, which is introduced into the material model based on stress increments at each material point and the number of cycles. The fatigue damage evolution is integrated per number of cycles with no need to model each individual cycle. This approach allows to consider the additional crack growth that may result due to force redistribution during the fatigue damage evolution process. The current paper presents the improved version of the fatigue model published previously by the authors as well as their application of modelling the fatigue crack growth in concrete structures strengthened by Fiber Reinforced Polymer (FRP) composites. .

1 INTRODUCTION

This paper demonstrates an efficient approach for modelling high-cycle fatigue in concrete structures without the need of modelling every individual cycle. Fatigue crack propagation is a common issue in many concrete structures when subjected to cyclic loading. However, there are very few fatigue models available for use in conjunction with advanced concrete material models and nonlinear finite element analysis. The available models that are published in the literature, for instance [1] usually deal with the low level of fatigue cyclic loading. The needs of numerical nonlinear simulation analysis is important to investigate all levels of fatigue load application., considering thousands and millions of cycles. The available models for high cycle fatigue [2] are usually based on

linear elastic fracture mechanics, and are not quite used for tracing the actual crack propagation. Such method cannot be easily extended for the finite element analysis using the smeared crack approach, which is by far the most used approach in commercial applications for practical analysis of concrete structures.

The three-dimensional fracture-plastic model [3] has been extended to capture fatigue damage in tension. The first version of the model has been presented in [4] and [5]. The current paper presents the improved version of the fatigue model as well as its application of modelling the fatigue crack growth in concrete structures strengthened by FRP anchorage application.

The material model is based on the classical S-N or Wöhler curve. The S-N criterion is

translated into a material damage, which is introduced into the material model based on stress increments at each material point and the number of cycles. The fatigue damage evolution is integrated per number of cycles without the need to model of each individual cycle. This approach allows to consider the additional crack growth that may result due to force redistribution during the fatigue damage evolution process.

The fatigue strength is an important factor in the design of infrastructures such as highways and railway bridges that subjected to repeated loadings by high speed railways or heavy trucks. Another typical structures, where fatigue is an important design criterion, are wind turbine support structures.

The fatigue model validation is demonstrated on an example of three point bending experiment from VUT Brno [6] and using an example of concrete strengthening.

Existing structures are often strengthened by various strengthening applications. One of the common solutions that widely used is the strengthening technique with FRP composite materials. This is due to the material performance of superior tensile strength, light weight, ease to install, and ability to resist harsh environmental conditions. The characteristics of FRP composite materials have significant influence on sustainability of infrastructures as it provided low emission to air and water when it compared to traditional material such as steel. The laminates and bidirectional fabric sheets can be bonded to the external surfaces of the strengthened structure. This process can be very fast with minimum disruption to its usage. Also the application of FRP laminates has a minimum effect on the structural dimensions.

The advanced method of non-linear finite element analysis can be used to verify the performance of the FRP strengthening system in concrete structures. The presented fatigue model herein this paper is used to simulate the fatigue strength of FRP anchorage system which includes Carbon FRP laminate and bidirectional sheets bonded to concrete surface. The simulation is compared with experimental results conducted at Swinburne

University of Technology in Australia [8]. A finite element model (FEM) was developed to verify the experimental result and obtain further insight of fatigue damage behavior and related parameters. The calibrated model showed successful correlation with the experimental results with regards to fatigue number of cycles and mode of failure.

2 MATERIAL PROPERTIES OF THE FATIGUE MODEL

The material model for the crack fatigue growth extends the fracture-plastic material model [3]. This model assumes for tensile fracture the total strain ε decomposition into the elastic ε_e and fracturing ε_f part.

$$\varepsilon = \varepsilon_e + \varepsilon_f \quad (1)$$

In the fracture-plastic material model, the crack growth is controlled by the internal parameter ε_{\max}^f , which represents the maximal fracturing strain reached during the cracking process at each crack.

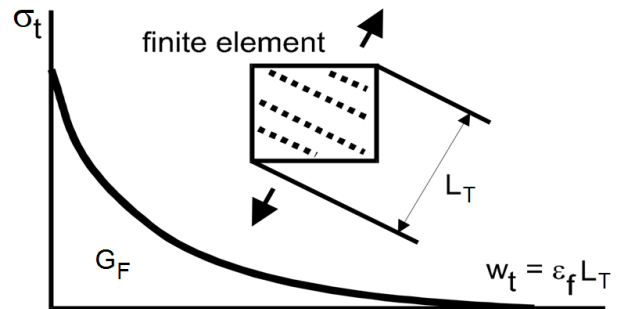


Figure 1: Softening law in tension.

This means that the current tensile strength at any time during the fracturing process can determined using the tensile softening law (Figure 1) as:

$$\sigma_t = f_t(w_{\max}), \quad w_{\max} = \varepsilon_{\max}^f L_t \quad (2)$$

Where σ_t represents the current tensile strength, w_{\max} is the maximal crack opening w_t reached during the loading process and L_t is the crack band size, which is based on the finite element size as shown in Figure 1. For the above softening law it is possible to define the following inverse relationship:

loading is then integrated numerically for a given number of fatigue intervals $k = n/\Delta n$.

$$\Delta w_{fat} = \sum_{i=1}^{k-1} \left\{ \frac{w_{fat}(\Delta n(i+1), \sigma_u^i, \sigma_b^i) - w_{fat}(i \Delta n, \sigma_u^i, \sigma_b^i)}{\Delta n} \Delta n + \frac{w_{fat}(i \Delta n, \sigma_u^i + \Delta \sigma_u^i, \sigma_b^i) - w_{fat}(i \Delta n, \sigma_u^i, \sigma_b^i)}{\Delta \sigma_u^i} \Delta \sigma_u^i + \frac{w_{fat}(i \Delta n, \sigma_u^i, \sigma_b^i + \Delta \sigma_b^i) - w_{fat}(i \Delta n, \sigma_u^i, \sigma_b^i)}{\Delta \sigma_b^i} \Delta \sigma_b^i \right\} \quad (11)$$

The fatigue algorithm involves the following steps in the nonlinear finite element analysis:

Algorithm 1:

- (1) Mark the start of the fatigue increment, save σ_b at all material points.
- (2) Perform fatigue loading up to the required upper load level. Then save σ_u at all material points.
- (3) Calculate and gradually apply damage due to n cycles in k steps as shown in (11).

After the application of the damage in step (3) of the above algorithm, the stresses at each material point are checked with respect to the fracture-plastic material model. At this point, additional damage and cracking may be introduced due to the violation of the material cracking criteria [3]. The proposed algorithm is sensitive to the selected steps size Δn . Due to the redistribution of internal forces during the fatigue loading, the levels of the upper σ_u and base stress σ_b will be changeable. The change of the upper stress level σ_u is taken into account in the step (3) of the above algorithm. To consider the gradual changes of the lower stress σ_b levels, it is recommended to unload the model to the base load levels during the fatigue loading process, and repeat the steps (1) and (2) in the above algorithm.

3 DIRECT TENSION EXAMPLE

This section demonstrates one of the example validation problems used to verify the proposed model. This example is a three-point bending beam tested at VUT Brno [6]. The photo of the experimental setup is shown in Figure 3. The specimen dimensions were 400 mm (length) \times 100 mm (height) \times 100 mm (depth), supports distance 300 mm, notch depth 10 mm. The finite element model used to simulate the fatigue strength is shown in Figure 4. Two sets of specimens were tested made of C30/37 and C45/55 class concrete.

The static response of the experiments was first used to calibrate the main material parameters such as tensile strength, fracture energy, etc.



Figure 3: Experimental setup of the three-point bending experiments from VUT Brno [6].

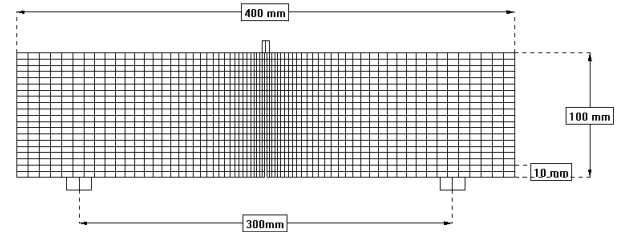


Figure 4: The finite element model for the validation three-point bending example.

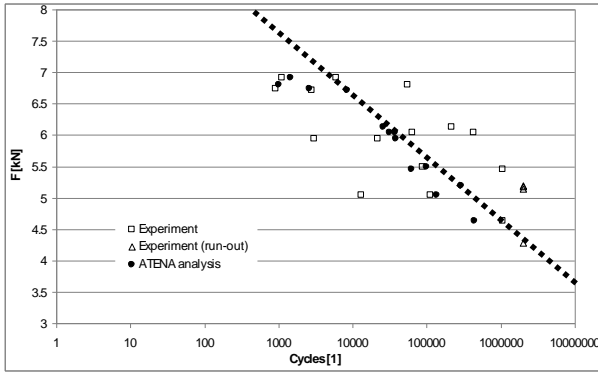


Figure 5: The comparison of the fatigue strength for the three-point bending validation example for C30/37.

The fatigue analysis was performed using the following approach:

1. loading up to the base load level (2 analysis steps)
2. storing the base stress σ_b
3. increasing the load to the upper stress level σ_u (18 analysis steps)
4. calculating the fatigue damage due to 10 cycles based on the difference between the stored and current stress and crack fields
5. introducing the damage into the material (10 analysis steps). The damage results in a displacement increase.
6. repeating steps 4 and 5 for increasing cycle counts until the model fails or two million total cycles are reached. The two million cycles were divided into 37 sets of increasing size (10, 10, 20, 30, 50, ..., 250 000, 300 000, 400 000, 400 000). In total, there were 380 analysis steps.
7. determining the number of cycles survived from the number of the last converged analysis step.

A parametric study was performed to determine the optimal values of β_{fat} . The optimal value was determined to be 0.08 for class 30/37 and 0.11 for class 45/55 concrete. These results are shown in Figure 5 and Figure 6 for class 30/37 and 45/55 concretes, respectively. The samples that did not fail in tests before reaching two million cycles (“run-out”) are marked by empty triangles. The comparison shows that the numerical model has clearly captured the mean values of the cycles until failure occurred, as observed in the experiment work.

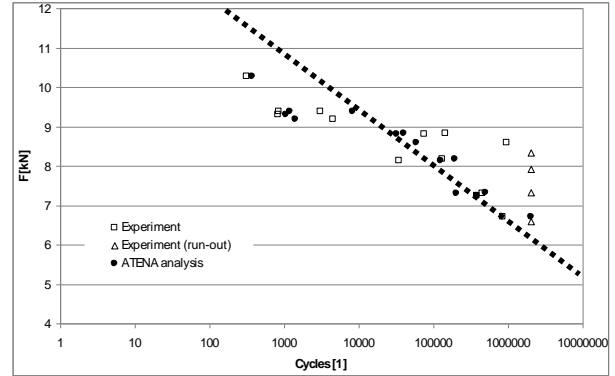


Figure 6: The comparison of the fatigue strength for the three-point bending validation example for C45/55.

4 MODELLING OF FRP STRENGTHENING TECHNIQUE

FRP has become a popular material for strengthening and rehabilitation of many concrete structures such as buildings and bridges. The material can be applied to structural elements as externally-bonded reinforcement to enhance their flexural, shear, axial and torsional strength.

The FRP material shows many advantages for strengthening purposes, however the bond behavior between the FRP application and concrete is the most challenging issue. In order to prevent the occurrence of debonding failure, various techniques have been explored such as the concept of FRP anchorage systems, which are summarized by Kalfat et al [7].

The anchorage strengthening system is selected as the second validation and demonstration problem for the presented fatigue model. This system was developed and experimentally tested at Swinburne University of Technology in Australia [8].

Figure 7 shows the test specimen with the developed anchor system. The experimental work carried out by [8] included reinforced concrete blocks with dimensions of 400×400×250mm as shown in Figure 8. The concrete block is placed into the testing machine as shown in Figure 9. The blocks are reinforced with four 12mm closed ties in each direction. The reinforcement has the spacing of 120mm and a cover of 30mm. The two larger faces of the concrete specimen (400x400mm) were sandblasted to achieve an

appropriate rough surface prior to apply the FRP-to-concrete bond application. Two layers of bi-directional fabric sheets with dimensions of 400 x 300mm were applied to the concrete surface, with a CFRP laminate placed between each fabric layer. The first fabric layer was saturated with resin and applied to the concrete using a wet lay-up technique. The next step involved applying the FRP laminate over the first layer of bidirectional fabric sheet using laminate adhesive. Lastly, the second layer of bidirectional fabric sheet was applied over the top of the FRP laminate. This arrangement is replicated in the FEM model as shown in Figure 10.

Figure 11 shows the finite element mesh used in the numerical simulations. First the static tests were analyzed. In these tests the specimens were subjected to tensile static loading up to failure to establish the cyclic loads corresponding to stress ranges of 20-70%, and 20-60% of the average static test failure load. The load-displacement curves obtained by this investigation are shown and compared in Figure 12. The static tests are also used to determine and validate the material to be used in the numerical simulations. A summary of material properties used in this experimental and FEM validations are listed in Table 1. The calculated strength of the static test obtained by FEM is about 148kN, which close the average experimental static test results of 160kN. Very brittle failure was captured similar to the experimental observations, where it was not possible to have a stable control of the load after the peak was reached. The mode of failure captured in the FEM showed similar failure pattern observed in the experiment test. Figure 13 to Figure 15 shows the evolution of the bond failure at various load levels. In the proposed numerical model, the bond failure is modeled by crack propagation in the surface layer of concrete right below the first fabric layer.

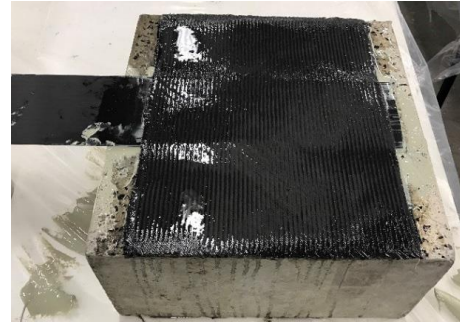


Figure 7: The view of the specimen preparation before the test.

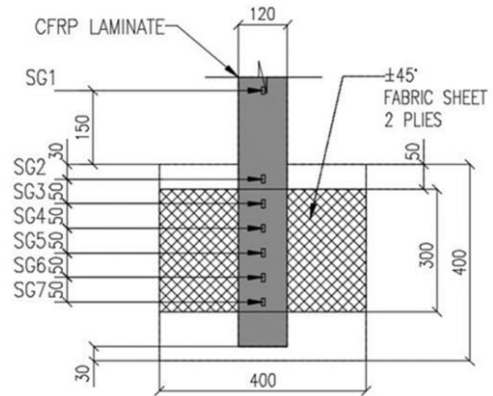


Figure 8: The geometry of the concrete specimen with FRP application.



Figure 9: The concrete specimen inside the testing machine.

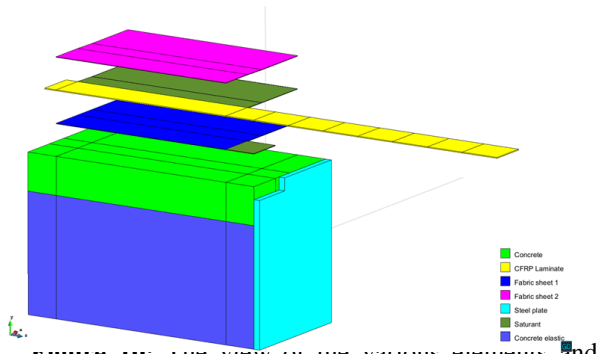


Figure 10: The view of the various elements and layers in the calibrated numerical model.

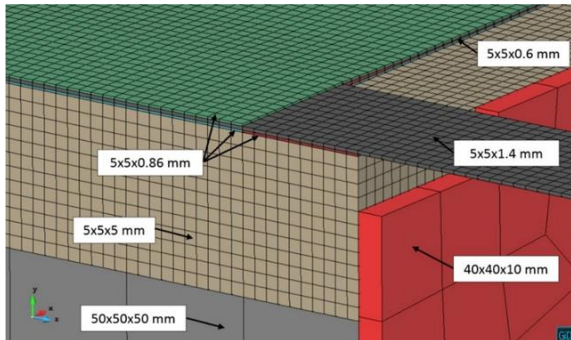
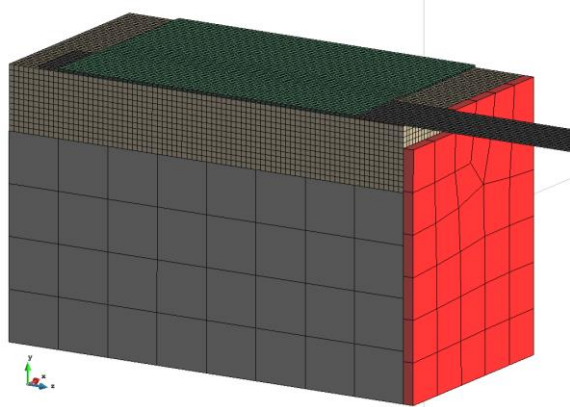


Figure 11: Mesh size configuration of anchored model.

This assumption shows good agreement with the observed behavior, where failure was occurred in the concrete surface layer and not in the bond or fabric layers. The static tests were used to validate this assumption. This assumption enabled the proposed fatigue model, to further develop the fatigue tensile cracking of concrete, to the simulation of the fatigue model of FRP anchorage strengthening method. In this approach, the fatigue failure of the bonding mechanism is simulated by the fatigue cracking of the concrete top surface layer.

The fatigue simulation was performed using the fracture-plastic material model and the

fatigue model described in Section 2. The fatigue analysis follows the process described in Section 2 in Algorithm 1. The model is first loaded up to the base level as indicated in Table 2. After that, the upper stress level in all integration points is stored.

Table 1: Material parameters used in the experimental and simulation work

Property	Concrete model	CFRP Lamin.	Satur.	Bi-dir. FRP
Comp. str. f_c [MPa]	31.6	-	-	-
Tensile str. f_t [MPa]	2	2906	68	3790
Elastic m. E [GPa]	33.3	181	>3.0	230
Poisson ν	0.2	0.42	-	-
Fract. engr. G_F [N/m]	80	-	-	-
β_{fat}	0.15	-	-	-

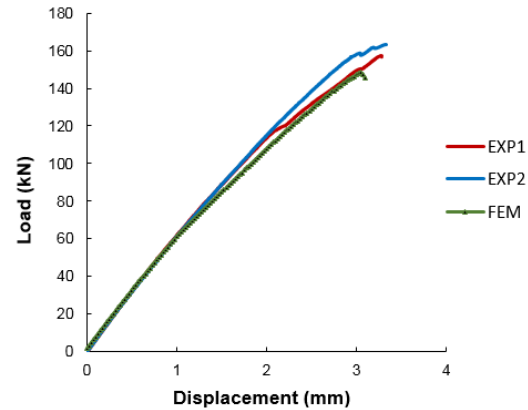


Figure 12: The comparison of load-displacement curves for Static test analysis.

Then the fatigue damage is evaluated and applied gradually using the equation(11). The fatigue calculation and application follows in a number of predefined steps, which allows the force redistribution to take place and upper and bottom stress levels σ_b and σ_b are gradually updated

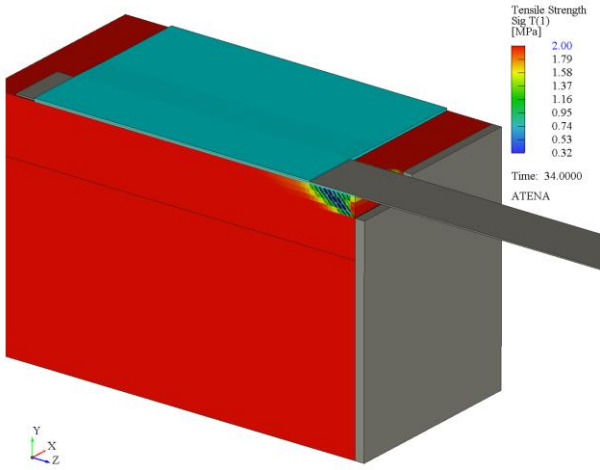


Figure 13: Static test at 51.5kN, cracks > 0.01 mm

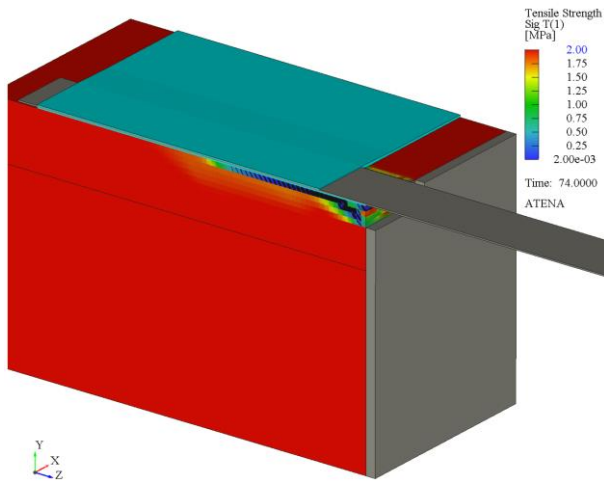


Figure 14: Static test at 100kN, cracks > 0.05 mm

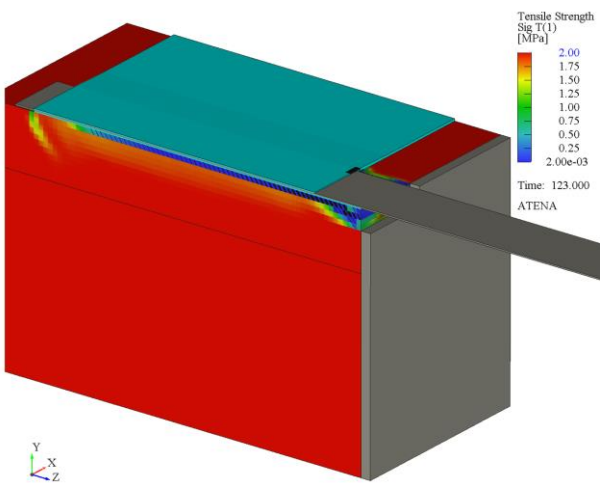


Figure 15: Static test at peak 148 kN, cracks > 0.05 mm

Table 2: Summary of fatigue results for the FRP anchored example.

Test ID	Stress Ratio [%]	Load range [kN]	Experiment		FEM β_{fat} 0.15 (mil.)
			no of cycles at failure (mil.)	no of cycles stopped without fail. (mil.)	
AF1	20-70	32112	1.355		1.0
AF1-R			0.607		
AF2	20-60	32-96		5.6	7.6
AF2-R				4.0	

R: Repeated

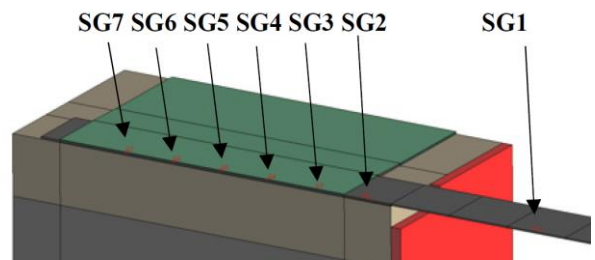


Figure 16: Strain gauge configurations.

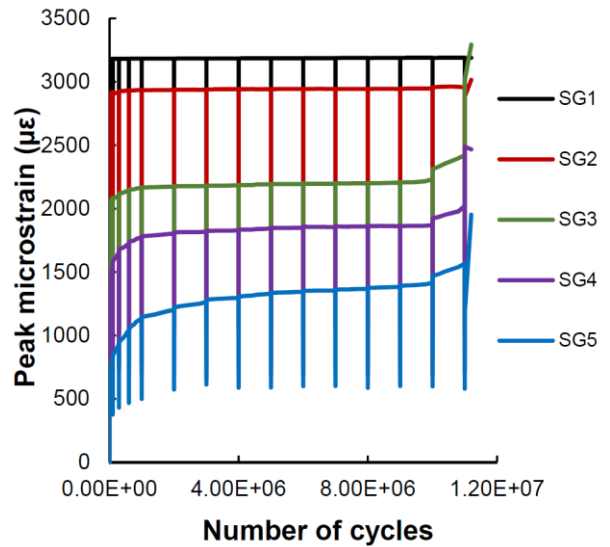


Figure 17: Strain gauge evolution in the strain monitors during the fatigue loading.

The fatigue test results are summarized in Table 2. The main parameter to compare is the number of cycles to failure. Overall four fatigue tests were performed for two load level intervals: 20-70% and 20-60%.of the ultimate

static failure load For each load interval two tests have been performed.

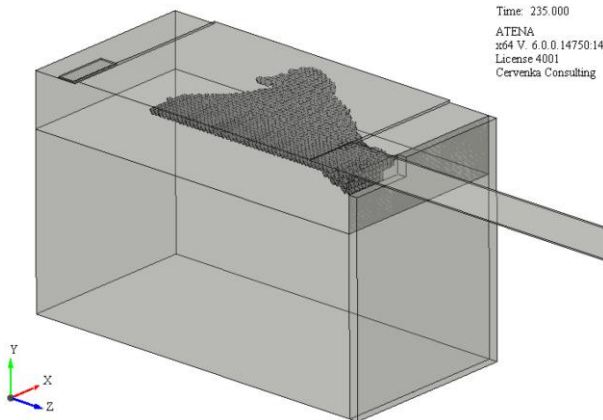


Figure 18: Crack pattern before failure in the fatigue test.

For the first interval 20-70%, the two fatigue tests were failed after 1.355 and 0.607 million cycles respectively. For the second load interval 20-60%, no fatigue failure was observed for the two repeated tests. Hence, the tests were terminated after 5.6 and 4 million cycles, respectively. The fatigue failure loads obtained from the numerical simulations are listed in the last column of Table 2. Good correlation was obtained when using the fatigue parameter of $\beta_{fat} = 0.15$. This represents a realistic value, since for typical concrete β_{fat} values are in the range of 0.06-0.08. In FRP strengthening, the bond strength is governed by the thin surface layer of concrete, which can be expected to have much lower fatigue strength, i.e. higher value of β_{fat} . The numerical simulation is used to provide further insight into the system behavior during the fatigue crack propagation by predicting the fatigue life performance and mode of failure captured by the strain gauge monitors in the FEM (see Figure 16 and Figure 17). Typical crack pattern at the time of failure is shown in Figure 18. The mode of failure observed in the calibrated fatigue model showed good agreement with experimental test investigation. Figure 19 shows the experimental failure of the anchored model under cyclic loadings. It can be noticed that the failure occurred in the concrete cover with full separation of the patch anchors from the concrete surface. No slippage of the laminate was observed between the two fabric sheets, which confirmed that good bonding was achieved.



Figure 19: Mode of failure of the anchored model observed in the experimental work.

5 CONCLUSIONS

This paper presents a fatigue model that was developed for high cycle fatigue assessment of concrete structures by non-linear finite element method. The objective of the model is to enable the assessment of structures that subjected to high cycle fatigue loading, when thousands and millions cycles are taken into account without the need to analyze each cycle. On the other hand, the model enables to consider the redistribution of forces, which must occur during the crack propagation process.

Several validation problems are presented in Section 3 for three point bending fatigue concrete tests with a notch and in Section 4 for fatigue bond failure of concrete structure strengthened by FRP applications.

The model shows good agreement with the experimental test results. The calibrated finite element model demonstrated practical use of the fatigue damage model for strengthening and retrofitting concrete structures with FRP composite materials

The presented models and analyses have been developed during the Eurostars research project "BIM based Cyber-physical System for Bridge Assessment" funded by Ministry of Youth and Education of Czech Rep. no. 7D17001.

REFERENCES

- [1] Hordijk D A. Local approach to Fatigue of Concrete. PhD thesis, Delft University of Technology; 1991.
- [2] Slowik W, Plizzari G, Saouma, V E. Fracture of concrete under variable amplitude fatigue loading. *ACI Materials Journal*; 1999.
- [3] Cervenka J, Papanikolaou V K. Three Dimensional Combined Fracture – Plastic Material Model for Concrete. *Int. Journal of Plasticity*, Volume 24, Issue 12, December 2008, ISSN 0749-6419.
- [4] Pryl, D., Cervenka, J., and Pukl, R., 2010, 'Material model for finite element modelling of fatigue crack growth in concrete', *Procedia Engineering*, vol. 2, no. 1, pp. 203-212
- [5] Pryl, D, Mikolášková, J and Pukl, R, 2014, 'Modeling fatigue damage of concrete', *Key Engineering Materials*, vol. 577, pp. 385-388.
- [6] Seitzl, S. & Keršner, Z., 2012. The fatigue crack growth in ce-ment based composites: Experimental aspects. IALCCE 2012.
- [7] Kalfat, R. Al-Mahaidi, S.T. Smith, Anchorage Devices Used to Improve the Performance of Reinforced Concrete Beams Retrofitted with FRP Composites: A State-of-the-Art Review, *Journal of Composites for Construction* 17(1) (2013) 14-33.
- [8] Al-Saoudi, R. Al-Mahaidi, R. Kalfat, J. Cervenka, 2019, Finite element investigation of the fatigue performance of FRP laminates bonded to concrete, *Composite Structures*, Vol. 208, pp. 322-337